LETTERS
PUBLISHED ONLINE: 8 MAY 2011 | DOI: 10.1038/NNANO.2011.64
nature nanotechnology

Quantum measurement and orientation tracking of fluorescent nanodiamonds inside living cells

L. P. McGuinness[1,2], Y. Yan[3], A. Stacey[1], D. A. Simpson[1,2], L. T. Hall[1,2], D. Maclaurin[1,2], S. Prawer[1], P. Mulvaney[4], J. Wrachtrup[5], F. Caruso[3], R. E. Scholten[1,6] and L. C. L. Hollenberg[1,2]*

Fluorescent particles are routinely used to probe biological processes[1]. The quantum properties of single spins within fluorescent particles have been explored in the field of nanoscale magnetometry[2–8], but not yet in biological environments. Here, we demonstrate optically detected magnetic resonance of individual fluorescent nanodiamond nitrogen-vacancy centres inside living human HeLa cells, and measure their location, orientation, spin levels and spin coherence times with nanoscale precision. Quantum coherence was measured through Rabi and spin-echo sequences over long (>10 h) periods, and orientation was tracked with effective 1° angular precision over acquisition times of 89 ms. The quantum spin levels served as fingerprints, allowing individual centres with identical fluorescence to be identified and tracked simultaneously. Furthermore, monitoring decoherence rates in response to changes in the local environment may provide new information about intracellular processes. The experiments reported here demonstrate the viability of controlled single spin probes for nanomagnetometry in biological systems, opening up a host of new possibilities for quantum-based imaging in the life sciences.

The extension of fluorescence imaging to modalities other than pure spatial imaging has enabled real-time detection and monitoring of previously inaccessible, but important cellular processes. The dynamics of molecular motors[9], protein diffusion[10] and changes in ion concentration[11] have all been elucidated by adding extra functionality to conventional fluorescence microscopy. With the ability to monitor the quantum state of fluorescent atomic systems, additional information about measurable properties intrinsic to the probe or local environment can now be acquired through emerging quantum sensing technologies. This capability has potential for electromagnetic sensing of the cellular environment, such as in neuronal networks, ion channel activity[12] and embryological development[13]. Here, we demonstrate quantum measurement of single fluorescent atomic centres in nanodiamonds taken up endosomally by HeLa cells, enabling improved spectral identification and orientation tracking, with potential for sensitive nanoscale magnetometry.

At the confluence of quantum metrology and biology, the nitrogen-vacancy (NV) centre in diamond has emerged as a leading contender for quantum sensing applications. These atomic centres display a remarkable range of properties, including sustained fluorescence, allowing detection at the single molecule level[14], and long quantum coherence times under ambient conditions[15]. Furthermore, diamond nanocrystals have proven biocompatibility[16,17]. Nanoscale magnetometry using single NV spins[4,5,18] has been performed in non-biological environments[2,3], with sensitivities down to 4 nT $Hz^{-1/2}$ for oscillating fields[15] and wide field imaging sensitivity at 20 nT $Hz^{-1/2}$ (ref. 19). In principle, improved sensitivities can be achieved using multi-pulse-magnetometry[20,21]. For random magnetic field fluctuations in biological contexts, it has been shown that probing the quantum decoherence time of the NV system *in situ*[7,8] could enable direct non-invasive monitoring of single ion-channel function[12].

Although nanodiamonds containing NV centres have been introduced into cells as fluorescent markers[22–25], *in situ* monitoring of their quantum properties has not been demonstrated. This challenge raises several questions. Is it possible to perform a quantum measurement on nanodiamonds in living cells, requiring non-invasive measurement and control of the probe's quantum state? Is it possible to measure an effect of the intracellular medium on the NV system? Is quantum measurement sensitive to the motion of the probe in the cell? The proof-of-principle experiments reported here demonstrate that the combination of high-precision fluorescent tracking and quantum monitoring is compatible with cell viability, that quantum coherence is maintained within the complex electromagnetic intracellular environment, and that a quantum probe can provide valuable new information about the dynamics of the probe's motion and potentially its intracellular surroundings.

The NV centre is an atomic-sized defect, with stable fluorescence observed in crystals as small as 5 nm (ref. 26). Comprising a substitutional nitrogen atom and adjacent vacancy, the centre has a magnetically sensitive ground-state triplet, with the spin-zero level ($|0\rangle$) separated from the degenerate spin-one levels ($|\pm1\rangle$) by a microwave transition of 2.87 GHz owing to the diamond crystal field[27]. This splitting also defines a quantization axis along the $\langle 111 \rangle$ crystallographic direction, providing an intrinsic compass that can be monitored by means of quantum measurement. Readout of the quantum state is based on optically detected magnetic resonance (ODMR), a fluorescence measurement involving microwave spectroscopy to control the NV spin while monitoring fluorescence intensity, which varies depending on which state ($|0\rangle$, $|+1\rangle$ or $|-1\rangle$) is populated[14].

In this work, we describe three specific investigations that include measurement of the NV quantum state within living HeLa cells in culture (see Methods). In Study 1 we show how microwave spectroscopy can distinguish NV centres with otherwise identical fluorescence within the cell. Study 2 presents the first intracellular quantum coherence measurement of single spin systems, including Rabi and spin-echo sequences, providing a foundation for further intracellular magnetometry studies. In Study 3 we demonstrate a robust and precise method for orientation tracking of nanodiamonds in the intracellular medium, based on continuous ODMR monitoring.

[1]School of Physics, University of Melbourne, Victoria 3010, Australia, [2]Centre for Quantum Computation and Communication Technology, School of Physics, University of Melbourne, Victoria 3010, Australia, [3]Centre for Nanoscience and Nanotechnology, Department of Chemical and Biomolecular Engineering, University of Melbourne, Victoria 3010, Australia, [4]School of Chemistry and Bio21 Institute, University of Melbourne, Victoria 3010, Australia, [5]3. Physikalisches Institut, Universität Stuttgart, Pfaffenwaldring, D-70550 Stuttgart, Germany, [6]Centre for Coherent X-ray Science, School of Physics, University of Melbourne, Victoria 3010, Australia. *e-mail: lloydch@unimelb.edu.au

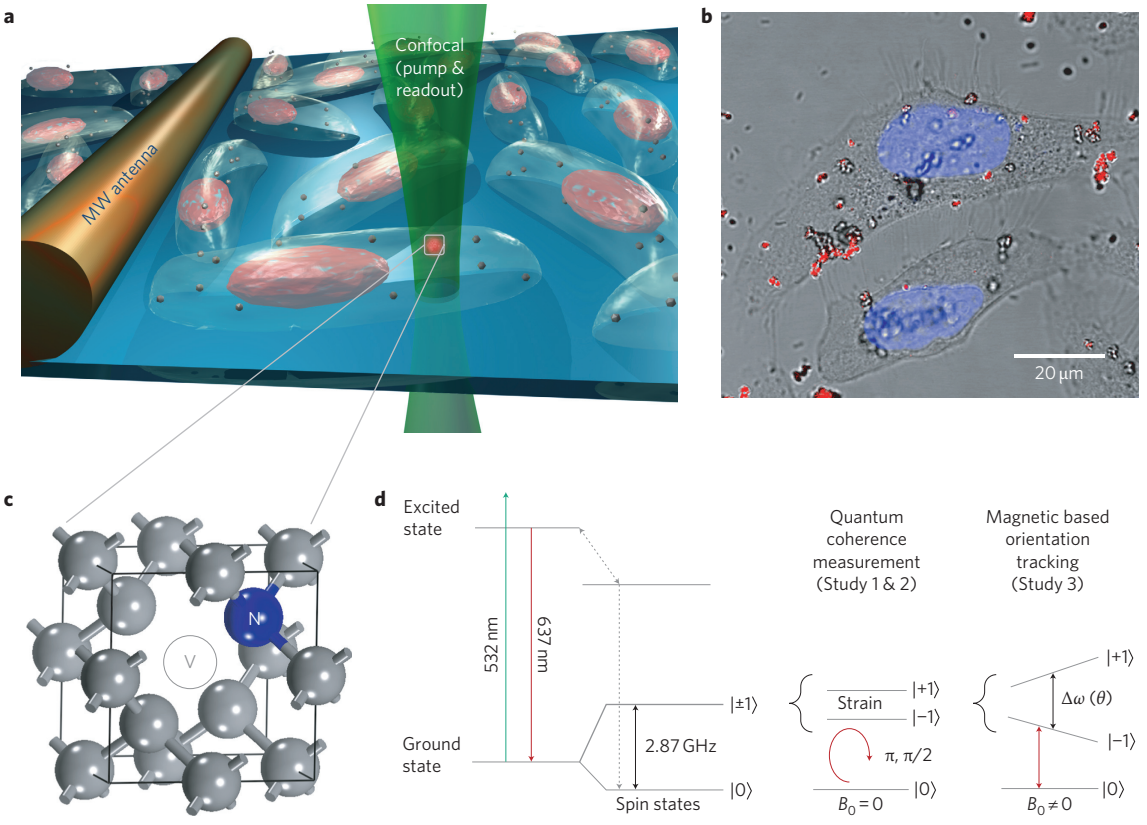

Figure 1 | Quantum measurement of single spins in living cells. a, Experimental setup, including microwave (MW) control of the NV spin levels and confocal fluorescence readout. **b**, Overlay of bright-field and confocal fluorescence images of HeLa cells, showing uptake of nanodiamonds. NV fluorescence is shown in red and the nucleus is stained with Hoechst 33342 (blue). Images were obtained on a Leica TCS SP2 confocal microscope. **c**, Atomic lattice structure of the NV centre. **d**, Quantum measurement and control of the NV centre. Left: energy levels of the NV probe system and fluorescence dynamics. Middle: quantum control for Studies 1 and 2 (π and $\pi/2$ pulses for spin-echo). Right: orientation-dependent Zeeman splitting $\Delta\omega(\theta)$ in an applied magnetic field B_0, measured in Study 3.

The experimental setup, shown in Fig. 1a, consists of a confocal microscope with microwave control. In Study 1 we first demonstrate how the unique quantum properties of each NV in the absence of an externally applied magnetic field ($B_0 = 0$) can be used as a fingerprint in the intracellular environment to spectrally separate nanodiamonds. HeLa cells cultured in media containing fluorescent nanodiamonds (Fig. 1b) were washed in phosphate buffered saline (PBS) before imaging (see Methods). Figure 2c shows a typical confocal image of one cell (HeLa-1), which contains two single NV centres (NV-1a and NV-1b) in the same focal plane. Their measured ODMR spectra are presented in Fig. 2a,b, which shows that under these conditions the respective centres have a unique strain signature. We use this technique to identify and track the optical emission from the NV centres, with the exceptionally stable fluorescence allowing localization with a precision of 20 nm over long timescales compared with the life of the cell (see Supplementary Information). Importantly, we find that the same ODMR spectrum is obtained over long periods, and is unaffected by nanodiamond movement within the cells. Our observations indicate that, by using nanodiamonds with a higher ^{13}C concentration, up to 1×10^4 centres can be uniquely identified (see Supplementary Information), which represents a substantial improvement over current methods used to spectrally discriminate fluorophores based on fluorescence (such as multicolour microscopy and linear unmixing[28]). The unique identification of nanoparticles over long timescales is of particular interest in applications where continuous tracking analysis is unfeasible or may be interrupted (for example, for tracking the fate of nanoparticles *in vivo*, tracking numerous nanoparticles in distinct locations or investigations of membrane motility, transport and mitotic events).

In Study 2 we demonstrate coherent quantum control and measurement of the spin state of the NV probe in the intracellular environment. A critical aspect of nanoscale magnetometry is the measurement and monitoring of the coherence time (T_2) of the NV probe, which is itself sensitive to magnetic fluctuations in the local environment[8,12,29], and/or specific molecular targets that may be driven externally. By tuning the microwave (MW) frequency to the $|0\rangle \rightarrow |+1\rangle$ resonance for NV-1a (and $|0\rangle \rightarrow |-1\rangle$ for NV-1b) we induce and detect coherent Rabi transitions between the quantum states of each NV system (Fig. 3a,b). Coherence times for both NV-1a and NV-1b were then measured by means of spin-echo, and this sequence was repeated for each NV as the cell timeline progressed (see Supplementary Information). This demonstration in a living cell represents the full suite of quantum control and measurement required for nanoscale intracellular magnetometry.

Figure 3c plots the initial spin-echo envelopes, and shows that NV-1a experiences faster overall decoherence (including intrinsic crystal and external sources) than NV-1b. The coherence time T_2 is dominated by interactions with internal crystal spins, unpaired spins on the nanodiamond surface and magnetic fluctuations in the local intracellular environment. At the 13 h time point, we observe a drop in the decoherence rate for NV-1b (at 95% confidence level) indicating that a change in its nanoscale environment occurred (Fig. 3d). This change, occurring in conjunction with a degradation in the integrity of the cell nucleus and increased auto-fluorescence, can only be owing to an alteration in spin

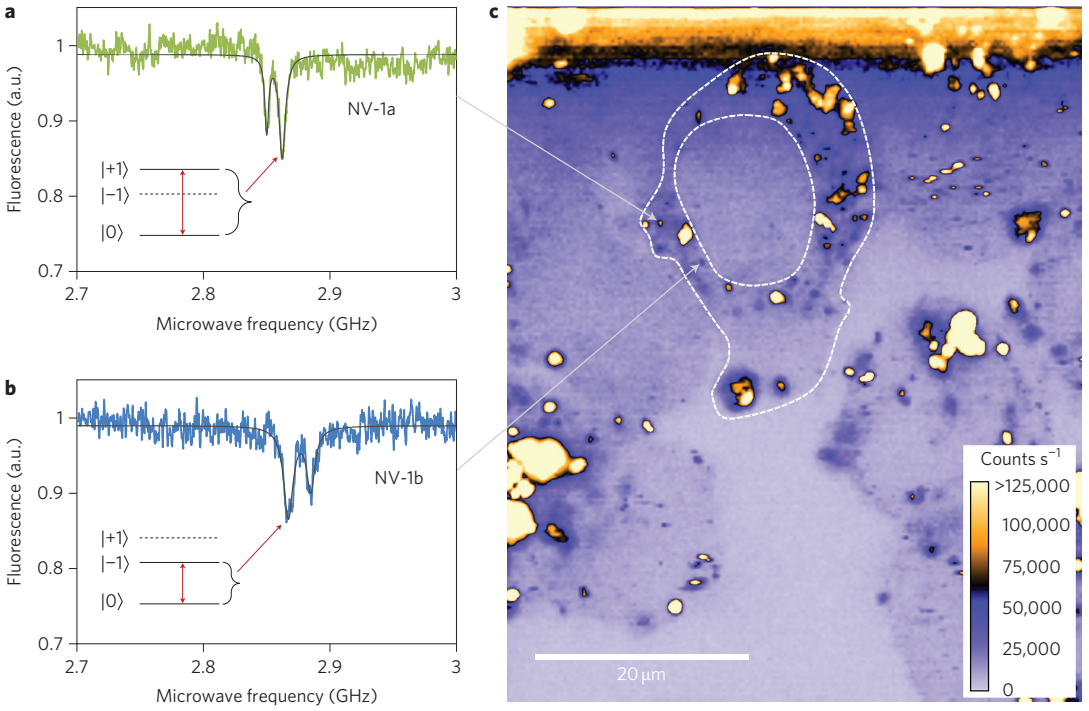

Figure 2 | Confocal image of a HeLa cell containing two isolated nanodiamonds with single NV centres and their measured ODMR spectra. a–c, Confocal image of HeLa-1 (**c**, $z = 11$ μm above the cover glass; edge of the microwave antenna cladding is visible at the top of the image), with fluorescence gated around the NV emission (650–800 nm). The nucleus and cell membrane are indicated with dashed lines for clarity. The optically detected magnetic resonance (ODMR) spectra of NV-1a (**a**) and NV-1b (**b**) show the different strain splitting between the two centres.

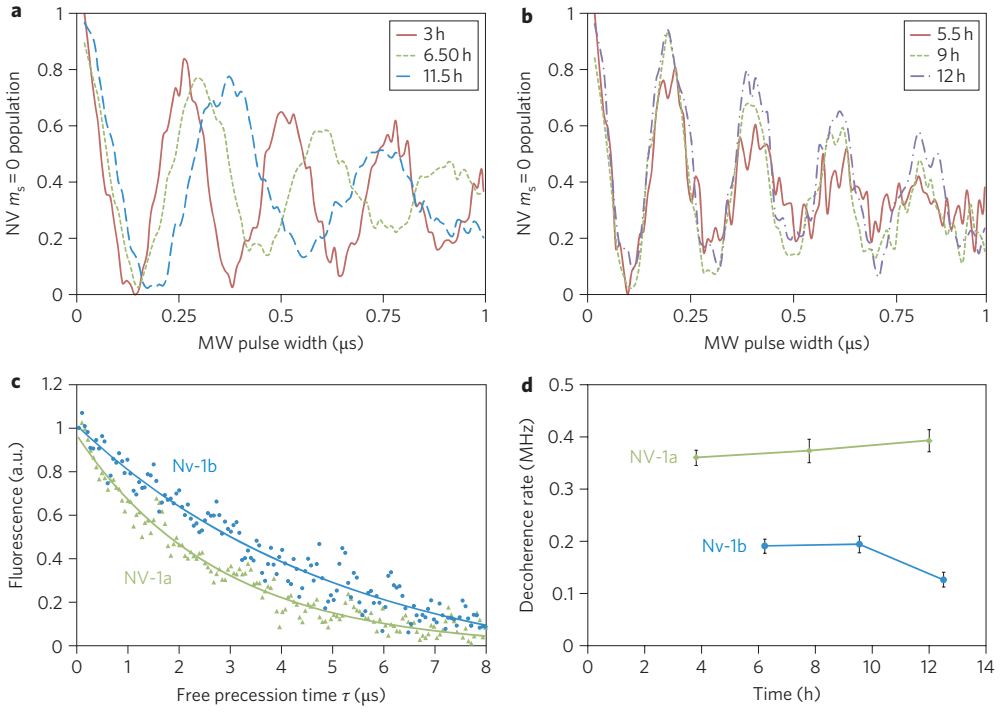

Figure 3 | Quantum coherence properties of the probes NV-1a and NV-1b in HeLa-1. a,**b**, Rabi oscillations of NV-1a and NV-1b measured at various times during the lifetime of the cell. **c**, Initial spin-echo measurements on both NV centres (statistical errors are at the 1% level). **d**, Time evolution of the decoherence rates extracted from the spin-echo profiles for both NV centres. The uncertainties in the extracted values, quoted at the one sigma level, are determined from the fit to the data.

dynamics at the nanodiamond surface or surrounding medium, and may be linked to production of unpaired electron species such as superoxide radicals, known to be generated during apoptosis[30]. Increased sensitivity to the environment can be achieved through the use of smaller nanodiamonds, multiple NV ensemble probes and multi-pulse quantum control techniques[20], coupled with improvements in the measurement timescale. Quite apart from proving the feasibility of quantum measurements on single spins

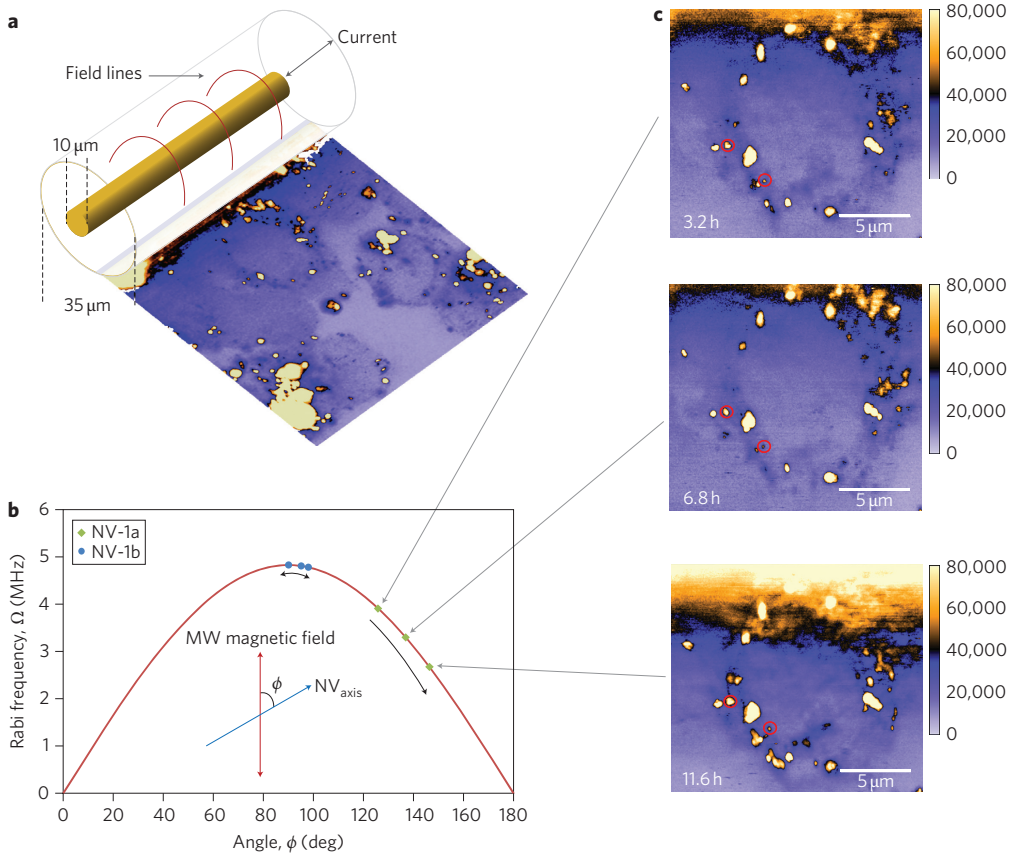

Figure 4 | NV axis rotation owing to motion of the nanodiamonds in HeLa-1. a, With constant MW power, the Rabi frequency is governed by orientation ϕ of the NV axis with respect to the MW driving field. **b**, Upper bounds on the change in orientation of the nanodiamonds based on a maximum initial perpendicular alignment of the higher Rabi frequency centre (NV-1b) with the MW field (see Supplementary Information). **c**, Confocal scan sequence showing the corresponding morphological changes in the cell during the same timeframe.

in a biological environment, the coherence measurements reported here set the stage for statistical studies exploring the link between measured quantum decoherence of the probe and local magnetic fluctuations, to provide new information about the underlying biological processes of interest.

To complete Study 2, we analysed the Rabi period as a function of time to gain information about the probe rotation. Throughout all the experiments, the delivered MW power was held constant, yet Fig. 3a,b shows that the two probes have dramatic differences in their respective Rabi frequency evolution. This variation arises owing to orientation-dependent coupling between the polarized microwave field and the NV magnetic dipole (Fig. 4a). For a rotating NV, the Rabi frequency Ω is given by $\Omega(\phi) = \Omega_0 \sin\phi$, where ϕ is the angle between the MW polarization and NV axes, and Ω_0 is the Rabi frequency for perpendicular alignment (see Supplementary Information). The higher Rabi frequency of NV-1b can be attributed to a well-aligned axis, and we use this to obtain an upper bound for the rotation by taking $\Omega = \Omega_0$ in the reference measurement. These estimates indicate a net rotation of NV-1a and NV-1b of up to 20° and 10°, respectively, during the course of the experiment (Fig. 4b,c).

Although a changing Rabi period provides information on the rotational motion of internalized nanodiamonds, the long timescale (hours) of this measurement limits its use for particle tracking. In Study 3, we demonstrate that continuous ODMR monitoring in the presence of an external magnetic field allows rotational motion of an internalized nanodiamond to be measured over millisecond acquisition timescales. A uniform magnetic field ($B_0 = 3.6$ mT) was used to produce an orientation-dependent Zeeman shift[31] on the $|\pm 1\rangle$ levels of a single NV centre (NV-2) in cell HeLa-2 (in a separate cell culture to the previous studies). Unlike Study 1, which had zero background field, the ODMR spectrum in this case depends on the orientation of the NV quantization axis with respect to B_0. The rotational motion of NV-2 was monitored over 16 h by continuously monitoring changes of the ODMR peak positions (at 30 s intervals).

Figure 5a shows two spectra taken over the life of the cell, demonstrating that the timescale for rotational monitoring is essentially unlimited, depending only on the cell lifetime. With knowledge of the applied magnetic field strength B_0, the nanodiamond orientation can be determined through the geometric relationship $\theta = \cos^{-1}(\hbar\Delta\omega/\mu_{NV}B_0)$ where θ is the angle between B_0 and the NV axis, μ_{NV} is the magnetic moment of the NV centre, and $\Delta\omega$ is the peak separation between the ODMR transitions (Fig. 5a). The angular precision and orientation tracking timescale are governed by the number of points used in the Lorentzian fit, as shown in Table 1 down to a 13-point fit, which gives a precision of 0.9° over an acquisition time of 89 ms. Figure 5b tracks the value of θ derived from the measurement of $\Delta\omega$ over 16 h, showing that the 13-point fit captures the rotational motion very well compared to the full data set. Figure 5c plots the three-dimensional position and rotation of NV-2 over a 3 h period (indicated by the dashed vertical lines in Fig. 5b). The restricted translational motion is in agreement with previous studies on internalization of similarly sized nanodiamonds in HeLa cells[23], suggesting that the nanodiamond remains immobilized within a membrane-enclosed vesicle following endocytosis. Furthermore, our tracking also provides information on the nanodiamond orientation, which is confined within 10°, confirming its relative immobilization.

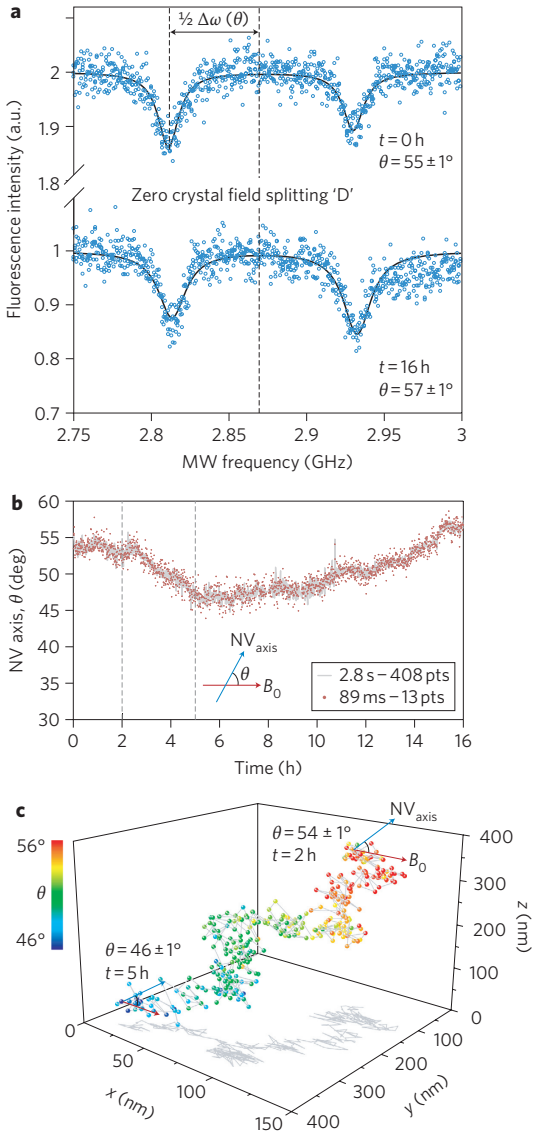

Figure 5 | Orientation tracking of NV-2 in HeLa-2. a, Changes in the orientation of the NV quantization axis relative to the external magnetic field owing to nanodiamond motion are manifest in the orientation-dependent Zeeman splitting $\Delta\omega(\theta)$ observed in the ODMR spectrum shown at various times over the HeLa-2 cell lifetime. **b**, Measured orientation of the nanodiamond as a function of time, and comparison of different acquisition rates. **c**, Four-dimensional tracking (position and orientation) of NV-2 in HeLa-2 over a 3 h period.

To quantify the potential of this new approach, we conducted an analysis of the shot noise statistics (see Supplementary Information). The results reveal that with modest optimization (fitting algorithm and field strength) the ODMR orientation tracking technique could resolve nanodiamond orientation to within 1° over a 3 ms acquisition interval. Such time resolution is necessary for understanding membrane nanomechanics and local viscosity in the cellular environment, and would allow real-time rotation monitoring of trafficking inside cells over long timescales, an important goal in intracellular nanoparticle tracking[32]. Alternatively, attachment of small (5 nm) nanodiamonds to the F_1-portion of ATP synthase would allow real-time monitoring of molecular rotation at the 10–100 ms timescale of ATPase activity. This compares well to the sensitivities obtained by reflection and fluorescence polarization microscopy[33–35], allows orders-of-magnitude longer tracking time than previous orientation measurements and, significantly, has been performed within the constraints of a living cell.

Table 1 | Scaling of temporal and orientational resolution determined from the number of ODMR data points used.

No. of points, *N*	Precision of θ (deg)	Acquisition time
408	0.3	2.85 s
204	0.4	1.43 s
102	0.5	712 ms
51	0.7	356 ms
26	0.8	178 ms
13	0.9	89 ms

The results presented here confirm that non-invasive quantum measurement is possible on nanodiamonds containing a single NV spin moving within living cells. As a consequence, we have demonstrated the techniques required for NV-based nanoscale biological magnetometry. Furthermore, unique imaging modalities not possible with conventional fluorescence microscopy emerge, including orientation tracking over long periods, with resolution in the millisecond timescale of intracellular events. Fluorescence detection and coherent control of single spins inside living cells is a significant milestone in the application of quantum techniques to further knowledge in the life sciences, and may ultimately play a role in the search for quantum coherence in biology[36].

Methods

Quantum measurements in living cells. Confocal imaging of the HeLa cells was performed through the cover glass, using an oil immersion lens ×100 (NA = 1.4). Cultured HeLa cells were adherent to the back surface of the cover glass, which was attached to the imaging mount. The cells were immersed in 3 ml PBS and kept at room temperature throughout the measurement. Confocal images at different depths were performed to identify the diamond nanocrystals that had been ingested by the cells. The NV centres characterized in this work were located several micrometres above the cover glass. Quantum measurements were carried out on single NV centres by applying a microwave signal along an insulated copper wire (diameter, 35 μm) located ~20 μm from the cells of interest. The two peaks observed in the ODMR spectrum (Fig. 2a,b) represent the transition frequency from the $|0\rangle$ to the $|-1\rangle$ and $|+1\rangle$ states, respectively. The observation of both peaks in the absence of an external magnetic field is attributed to localized strain present in the diamond nanocrystal. The quantum measurements carried out in this work were conducted on the transition exhibiting the highest fluorescence contrast. By applying a MW field resonant with a particular transition, the population of the spin states can be coherently driven between the $|0\rangle$ and the $|+1\rangle$ or $|-1\rangle$ states resulting in Rabi nutations. The Rabi and spin-echo measurements were implemented using a Spincore 500 MHz Pulse Blaster ESR-QuadCore card. The complete ODMR spectrum, as shown in Fig. 5, contains 1,000 points with an acquisition time of 7 ms per point. The position of the NV centre was tracked and optimized at 1 min intervals in Studies 1 and 2 and at 30 s intervals in Study 3. For orientation tracking, only 13 points around the lower peak are needed, giving an orientation acquisition time of 89 ms. The reflected light, fluorescence intensity and ODMR spectrum all provided evidence that a single NV in an isolated nanodiamond was addressed and tracked.

Cell culture and nanodiamond uptake. HeLa cells were cultured in Dulbecco's modified Eagle's medium (DMEM) supplemented with 10% fetal bovine serum and 1% penicillin/streptomycin. For cell uptake, type Ib non-detonation nanodiamonds with an average particle size of 45 nm (NaBond) were diluted in DMEM at a concentration of 20 μg ml^{-1}. The average particle size of the suspension before incubation was 140 nm (see Supplementary Information). HeLa cells were seeded on cover slips (4×10^5 cells per millilitre) and allowed to adhere overnight. Cells were then incubated with the DMEM:nanodiamond suspension for 3 h (37 °C, 5% CO_2). After treatment, the media was removed and the cells were washed (×3) with PBS. In all experiments, the low MW power applied resulted in no discernible difference in the morphology of cells adjacent to the MW wire compared with those at the edge of the field of view (an order of magnitude reduction in MW field strength). Separate control studies performed using propidium iodide as an indicator of cell death provided independent confirmation that HeLa cell viability is maintained at ~95% survivability rate over a 12 hour period in identical PBS room-temperature conditions (see Supplementary Information).

Received 31 January 2011; accepted 21 March 2011; published online 8 May 2011

References

1. Alivisatos, P. The use of nanocrystals in biological detection. *Nature Biotechnol.* **22,** 47–52 (2004).
2. Maze, J. R. *et al.* Nanoscale magnetic sensing with an individual electronic spin in diamond. *Nature* **455,** 644–648 (2008).
3. Balasubramanian, G. *et al.* Nanoscale imaging magnetometry with diamond spins under ambient conditions. *Nature* **455,** 648–651 (2008).
4. Chernobrod, B. M. & Berman, G. P. Spin microscope based on optically detected magnetic resonance. *J. Appl. Phys.* **97,** 014903 (2005).
5. Taylor, J. M. *et al.* High-sensitivity diamond magnetometer with nanoscale resolution. *Nature Phys.* **4,** 810–816 (2008).
6. Degen, C. L. Scanning magnetic field microscope with a diamond single-spin sensor. *Appl. Phys. Lett.* **92,** 243111 (2008).
7. Cole, J. H. & Hollenberg, L. C. L. Scanning quantum decoherence microscopy. *Nanotechology* **20,** 495401 (2009).
8. Hall, L. T., Cole, J. H., Hill, C. D. & Hollenberg, L. C. L. Sensing of fluctuating nanoscale magnetic fields using nitrogen-vacancy centers in diamond. *Phys. Rev. Lett.* **103,** 220802 (2009).
9. Forkey, J. N., Quinlan, M. E., Alexander Shaw, M., Corrie, J. E. T. & Goldman, Y. E. Three-dimensional structural dynamics of myosin V by single-molecule fluorescence polarization. *Nature* **422,** 399–404 (2003).
10. Sieber, J. J. *et al.* Anatomy and dynamics of a supramolecular membrane protein cluster. *Science* **317,** 1072–1076 (2007).
11. Miyawaki, A. *et al.* Fluorescent indicators for Ca^{2+} based on green fluorescent proteins and calmodulin. *Nature* **388,** 882–887 (1997).
12. Hall, L. T. *et al.* Monitoring ion-channel function in real time through quantum decoherence. *Proc. Natl Acad. Sci. USA* **107,** 18777–18782 (2010).
13. Funk, R. H. W., Monsees, T. & Özkucur, N. Electromagnetic effects—from cell biology to medicine. *Prog. Histochem. Cyto.* **43,** 177–264 (2009).
14. Gruber, A. *et al.* Scanning confocal optical microscopy and magnetic resonance on single defect centers. *Science* **276,** 2012–2014 (1997).
15. Balasubramanian, G. *et al.* Ultralong spin coherence time in isotopically engineered diamond. *Nature Mater.* **8,** 383–387 (2009).
16. Schrand, A. M. *et al.* Are diamond nanoparticles cytotoxic? *J. Phys. Chem. B* **111,** 2–7 (2007).
17. Chao, J. I. *et al.* Nanometer-sized diamond particle as a probe for biolabeling. *Biophys. J.* **93,** 2199–2208 (2007).
18. Maurer, P. C. *et al.* Far-field optical imaging and manipulation of individual spins with nanoscale resolution. *Nature Phys.* **6,** 912–918 (2010).
19. Steinert, S. *et al.* High sensitivity magnetic imaging using an array of spins in diamond. *Rev. Sci. Instrum.* **81,** 043705 (2010).
20. Hall, L. T., Hill, C. D., Cole, J. H. & Hollenberg, L. C. L. Ultrasensitive diamond magnetometry using optimal dynamic decoupling. *Phys. Rev. B* **82,** 045208 (2010).
21. de Lange, G. *et al.* Single-spin magnetometry with multipulse sensing sequences. *Phys. Rev. Lett.* **106,** 080802 (2011).
22. Chang, Y. R. *et al.* Mass production and dynamic imaging of fluorescent nanodiamonds. *Nature Nanotech.* **3,** 284–288 (2008).
23. Neugart, F. *et al.* Dynamics of diamond nanoparticles in solution and cells. *Nano. Lett.* **7,** 3588–3591 (2007).
24. Fu, C. C. *et al.* Characterization and application of single fluorescent nanodiamonds as cellular biomarkers. *Proc. Natl Acad. Sci. USA* **104,** 727–732 (2007).
25. Faklaris, O. *et al.* Photoluminescent diamond nanoparticles for cell labeling: study of the uptake mechanism in mammalian cells. *ACS Nano* **3,** 3955–3962 (2009).
26. Bradac, C. *et al.* Observation and control of blinking nitrogen-vacancy centres in discrete nanodiamonds. *Nature Nanotech.* **5,** 345–349 (2010).
27. Hossain, F. M., Doherty, M. W., Wilson, H. F. & Hollenberg, L. C. L. Ab initio electronic and optical properties of the N-V center in diamond. *Phys. Rev. Lett.* **101,** 226403 (2008).
28. Zimmermann, T., Rietdorf, J. & Pepperkok, R. Spectral imaging and its applications in live cell microscopy. *FEBS Lett.* **546,** 87–92 (2003).
29. Hanson, R., Dobrovitski, V. V., Feiguin, A. E., Gywat, O. & Awschalom, D. D. Coherent dynamics of a single spin interacting with an adjustable spin bath. *Science* **320,** 352–355 (2008).
30. Cai, J. & Jones, D. P. Superoxide in apoptosis. *J. Biol. Chem.* **273,** 11401–11404 (1998).
31. Epstein, R. J., Mendoza, F. M., Kato, Y. K. & Awschalom, D. D. Anisotropic interactions of a single spin and dark-spin spectroscopy in diamond. *Nature Phys.* **1,** 94–98 (2005).
32. Wittrup, A. *et al.* Magnetic nanoparticle-based isolation of endocytic vesicles reveals a role of the heat shock protein GRP75 in macromolecular delivery. *Proc. Natl Acad. Sci. USA* **107,** 13342–13347 (2010).
33. Chung, I., Shimizu, K. T. & Bawendi, M. G. Room temperature measurements of the 3D orientation of single CdSe quantum dots using polarization microscopy. *Proc. Natl Acad. Sci. USA* **100,** 405–408 (2003).
34. Rosenberg, S. A., Quinlan, M. E., Forkey, J. N. & Goldman, Y. E. Rotational motions of macromolecules by single-molecule fluorescence microscopy. *Acc. Chem. Res.* **38,** 583–593 (2005).
35. Kukura, P. *et al.* High-speed nanoscopic tracking of the position and orientation of a single virus. *Nature Meth.* **6,** 923–927 (2009).
36. Engel, G. S. *et al.* Evidence for wavelike energy transfer through quantum coherence in photosynthetic systems. *Nature* **446,** 782–786,(2007).

Acknowledgements

The authors thank F. Jelezko and A. Johnston for helpful discussions and advice, and S. Szilagyi for technical assistance. This work was supported by the Australian Research Council under the Centre of Excellence scheme (CE110001027), the Discovery Project scheme (DP0770715 and DP0877360), the Federation Fellowship Scheme (FF0776078) and the Baden-Wuerttemberg Foundation.

Author contributions

L.P.M., A.S., D.S. and R.E.S. designed and constructed the confocal/ESR system, performed the measurements and carried out the data analysis. Y.Y. and F.C. planned and conducted the cellular uptake experiments, and analysed the data. D.M., L.T.H. and L.C.L.H. carried out the theoretical analyses. L.C.L.H., J.W., F.C., P.M. and S.P. conceived and directed the project. L.C.L.H. wrote the paper with contributions from all authors.

Additional information

The authors declare no competing financial interests. Supplementary information accompanies this paper at www.nature.com/naturenanotechnology. Reprints and permission information is available online at http://www.nature.com/reprints/. Correspondence and requests for materials should be addressed to L.C.L.H.